A comparison of edge turbulence in tokamaks, stellarators, and reversed-field pinches*

Cite as: Physics of Fluids B: Plasma Physics **5**, 2491 (1993); https://doi.org/10.1063/1.860734
Submitted: 30 November 1992 . Accepted: 11 February 1993 . Published Online: 04 June 1998

H. Y. W. Tsui, A. J. Wootton, J. D. Bell, R. D. Bengston, D. Diebold, J. H. Harris, N. Hershkowitz, C. Hidalgo, J. C. Ingraham, S. J. Kilpatrick, G. X. Li, H. Lin, D. M. Manos, M. A. Meier, G. M. Miller, C. P. Munson, J. Pew, S. C. Prager, Ch. P. Ritz, A. Rudyj, K. F. Schoenberg, J. Sorensen, T. Tanaka, T. Uckan, and P. G. Weber

A comparison of edge turbulence in tokamaks, stellarators, and reversed-field pinches*

H. Y. W. Tsui,† A. J. Wootton, J. D. Bell,[a] R. D. Bengston, D. Diebold,[b] J. H. Harris,[a] N. Hershkowitz,[b] C. Hidalgo,[c] J. C. Ingraham,[d] S. J. Kilpatrick,[e] G. X. Li, H. Lin, D. M. Manos,[e] M. A. Meier, G. M. Miller,[d] C. P. Munson,[d] J. Pew,[b] S. C. Prager,[b] Ch. P. Ritz, A. Rudyj,[f] K. F. Schoenberg,[d] J. Sorensen,[b] T. Tanaka,[b] T. Uckan,[a] and P. G. Weber[d]
Fusion Research Center, University of Texas at Austin, Austin, Texas 78712

(Received 30 November 1992; accepted 11 February 1993)

Edge equilibrium, turbulence and transport related plasma parameters from the Advanced Toroidal Facility (ATF) [Fusion Technol. **10**, 179 (1986)] torsatron, the ZT-40M [Fusion Technol. **8**, 1571 (1985)] reversed-field pinch, the Phaedrus-T [Nucl. Fusion **32**, 2040 (1992)] tokamak, the Texas Experimental Tokamak (TEXT) [Nucl. Technol. Fusion **1**, 479 (1981)], and the Tokamak Fusion Test Reactor (TFTR) [in *Plasma Physics and Controlled Nuclear Fusion Research, 1990* (International Atomic Energy Agency, Vienna, 1991), Vol. 1, p. 9] have been obtained using a standardized Langmuir probe array and a consistent set of data analysis packages. Additional data from some other devices have also been furnished via private communications and incorporated from published results. Experimental results over a wide range of parameters are compared and the turbulence contribution to edge transport are assessed. Certain physical properties that are relevant to the modeling of edge turbulence are identified: namely, shear decorrelation of turbulence, the role of resistive dissipation and electron parallel thermal conduction, radial mode structure in sheared magnetic field, and electromagnetic contribution to the parallel Ohm's law.

I. INTRODUCTION

Understanding transport processes remains one of the central issues in fusion research.[1] Much experimental evidence exists to suggest that fluctuation-driven fluxes dominate particle and energy transport in magnetic confinement systems including tokamaks (e.g., Ref. 2 and references therein), stellarator,[3] and reversed-field pinches.[4,5] A major task in magnetic confinement physics is therefore to understand and to find ways to control these turbulence-induced fluxes. Comparative studies of edge turbulence and transport in different toroidal confinement systems[6–8] allow tests of theoretical predictions against experimental results over a wide range of parameters. To this end, a self-contained Langmuir probe diagnostic facility[9] equipped with its own data acquisition electronics and data analysis package has been deployed in collaborative measurements[3,10–12] in various devices including the Advanced Toroidal Facility[13] (ATF) torsatron, the ZT-40M[14] reversed-field pinch, the Phaedrus-T[15] tokamak, the Texas Experimental Tokamak[16] (TEXT) (and the upgrade TEXT-U), and the Tokamak Fusion Test Reactor[17] (TFTR). Additional data from some other devices have also been incorporated from published results or furnished via private communications.

In this study we focus on fluctuations observed with Langmuir probes. Although these fluctuations are not necessarily composed of purely "electrostatic" modes, the transport associated with them is often labeled as "electrostatic" so as to distinguish it from the transport associated with stochastic magnetic fields. Power loading on the probe tips limits probe measurements to within the scrape-off layer and the edge plasma up to a few cm inside the last-closed flux surface. The probe assembly is mounted on a fast reciprocating drive to minimize heating of probe tips and to provide simultaneous and local measurements of equilibrium and fluctuating (typically 1–500 kHz) electron temperature (T_e), density (n), and plasma potential (φ_{pl}), as well as turbulence-induced particle and electron energy fluxes. A rotating vacuum seal allows optimum alignment to preclude interference (shielding) between probe tips. The standardized four-pin probe array consists of two tips measuring the floating potential φ_{fl}, and the other two connected as a double-probe pair with sufficient bias voltage ($\geqslant 4T_e/e$) to measure the ion saturation current I_{sat}. In this way, the electron temperature can be obtained using a triple probe technique[18] with correction for phase delay[19] when necessary. Most of the data were acquired using this four-pin configuration. A modified triple probe technique[19] which utilizes a five-pin array has also been used in some cases to further reduce phase-delay error arising from finite probe tip separation across field lines. The two floating pins

*Paper 9I3, Bull. Am. Phys. Soc. **37**, 1591 (1992).
†Invited speaker.
[a]Permanent address: Oak Ridge National Laboratory, Oak Ridge, Tennessee 37831.
[b]Permanent address: University of Wisconsin—Madison, Madison, Wisconsin 53706.
[c]Permanent address: Centre de Investigaciones Energeticas, Medioanbientales y Tecnologicas (CIEMAT), Spain.
[d]Permanent address: Los Alamos National Laboratory, Los Alamos, New Mexico 87545.
[e]Permanent address: Plasma Physics Laboratory, Princeton University, Princeton, New Jersey 08544.
[f]Permanent address: Max-Plank-Institut für Plasmaphysik, D-8046 Garching bei München, Germany.

 0899-8221/93/5(7)/2491/7/$6.00

TABLE I. Generic differences in magnetic geometry of the three toroidal systems.

Parameter	Tokamak	Stellarator	RFP
Average curvature	good for $q>1$	good or bad	bad
Local curvature	good and bad	good and bad	bad
Magnetic shears	medium ($L_s \approx R$)	medium to 0	high ($L_s \approx a$)
	$dq/dr>0$	usually $dq/dr<0$	$dq/dr<0$
Plasma current density	medium	low to 0	high
Trapped particles	high, $\approx \sqrt{(2\epsilon)}$	high or low	low

are used for determining fluctuation characteristics utilizing a two-point cross-correlation technique.[20] These include estimates of the spectrum $S(k,\omega)$, and power weighted average values of perpendicular wave vector $\bar{k}_\perp$, frequency $\bar{f}$, phase velocity $V_{\rm ph}$, and width of the $\bar{k}_\perp$ spectrum $\sigma_{k_\perp}$. The fluctuation-driven particle flux $\Gamma_{\tilde{n}\tilde{E}}$ is derived from the cross-correlation between the density fluctuations $\tilde{n}$ and perpendicular electric field fluctuations $\tilde{E}_\perp$, i.e., $\Gamma_{\tilde{n}\tilde{E}}=\langle \tilde{n}\tilde{E}_\perp \rangle/B$ where $\langle \cdots \rangle$ denotes an ensemble average. The electron energy flux can be divided into a convective and a conductive component. The convective part is related to the particle flux by $Q_{T_e\tilde{n}\tilde{E}} = 5T_e\Gamma_{\tilde{n}\tilde{E}}/2 = 5T_e\langle \tilde{n}\tilde{E}_\perp \rangle/(2B)$ and the conductive part $Q_{n\tilde{T}_e\tilde{E}} = 5n\langle \tilde{T}_e\tilde{E}_\perp \rangle/(2B)$ can be determined from a correlation between $\tilde{T}_e$ and $\tilde{E}_\perp$. Many articles are available on the definitions of energy flux with a coefficient of either 5/2 or 3/2 (see, for example, Ref. 21). The difference is due to turbulence compression. It is important to note that proper correction for the electron temperature fluctuations $\tilde{T}_e$ is essential in these flux measurements. In contrast to the measurement of fluctuation level (rms value), the correction in the measurement of flux can be of order unity,[19] for instance, the value of uncorrected $\Gamma_{\tilde{n}\tilde{E}}$ can be negative in some situations.

The generic differences between device types are illustrated in Table I. They reflect the intrinsic properties of the equilibrium magnetic field configuration, e.g., magnetic shear and curvature and β. In the edge plasma, atomic processes such as impurity radiation and ionization can introduce additional instability drives.[22–25] In the scrape-off region where field lines are connected to material surfaces, instability can develop from surface dissipation[26,27] arising from the formation of a sheath. In these experiments, there are machine-specific differences in the edge conditions such as wall conditioning and limiter configuration. For instance, TEXT has a poloidal ring limiter, TFTR an inner toroidal belt limiter and both Phaedrus-T and TEXT-U have discrete limiters (which are segments of a poloidal ring). Table II summarizes some of the typical machine and edge plasma parameters.

II. VELOCITY SHEAR LAYER AND EDGE FLUCTUATIONS

A naturally occurring velocity shear layer has been found in tokamaks and stellarators, but has not yet been identified in RFP's. The layer exists in both divertor and limiter plasmas, is relevant to the study of edge turbulence because (i) it demarcates the plasma confinement zone from the scrape-off region, (ii) it affects the appearance of the fluctuations via a $\mathbf{E}\times\mathbf{B}$ Doppler shift in the observed frequency, and (iii) it can influence the turbulence via shear decorrelation. Formation of velocity shear layer has been associated with a number of mechanisms, e.g., the ion orbit loss,[28] the finite perpendicular momentum loss,[29] and the fluctuation-induced Reynolds stress.[30,31]

In Fig. 1 the velocity shear layers observed in some of these experiments are overlaid to illustrate the size scale. The layer is located close to, and its width can extend across, the last-closed flux surface. It is characterized by a peak plasma potential profile and a reversal in the phase velocity ($V_{\rm ph}$) of the turbulence. The phase velocity of the fluctuations is dominated by the equilibrium $\mathbf{E}\times\mathbf{B}$ rotation (i.e., $V_{\rm ph}\approx V_{\mathbf{E}\times\mathbf{B}}=E_r/B$) and the reversal of the propagation is related to the change in the radial electric field. In

TABLE II. Edge plasma parameters close to $r\approx a$ or the last closed flux surface. The average phase velocity $V_{\rm ph}$ is obtained from a two-point cross-correlation and $V_{\mathbf{E}\times\mathbf{B}}$ is the poloidal rotation derived from the equilibrium radial electric field.

Parameter	ATF	MST	ZT-40M	Phaedrus-T	TEXT	TFTR	Tokapole
a (m)	0.27	0.5	0.2	0.26	0.26	0.8	0.09
R (m)	2.1	1.5	1.14	0.93	1.0	2.45	0.5
B (m)	1	0.1	0.13	0.9	2	3.9	0.5
I_p (kA)	(ECRH)	250	120	90	200	900	12
$\lvert q_a \rvert$	1	0.03	0.02	3.4	3.3	6.5	3.5
$n(a)$ (10^{18} m^{-3})	1	3	10	3	2	0.5	10
T_e (eV)	25	35	25	40	30	100	20
L_n (cm)	4	1.5	2	3	3	9	1.7
L_{T_e} (cm)	12	>3	⩾8	2	3.5	11	3
$\lvert\tilde{n}\rvert/n$	0.05–0.1	0.2–0.4	0.3–0.5	0.2–0.3	0.1–0.2	0.3	0.16
$\lvert\tilde{T}_e\rvert/T_e$	0.05–0.1	0.1–0.25	0.2–0.4	0.1–0.2	0.05–0.1	0.1–0.2	
$e\lvert\tilde{\varphi}_{pl}\rvert/T_e$	0.2–0.4	~0.3	0.6–0.8	0.4–0.5	0.3–0.4	0.5–0.6	0.01
$\lvert V_{\rm ph}/V_{\mathbf{E}\times\mathbf{B}}\rvert$	⩾1		>1	⩾1	⩾1	⩾1	
$k_\perp$ (cm^{-1})	2	0.3	0.1	1.5	2.5	0.8	3
$k_\perp \rho_s$	0.1	0.2	0.1	0.1	0.1	0.02	0.3
$\Gamma_{\tilde{n}\tilde{E}}$ (10^{21} m^{-2} sec^{-1})	0.02	1	7	1	0.5	0.06	0.5

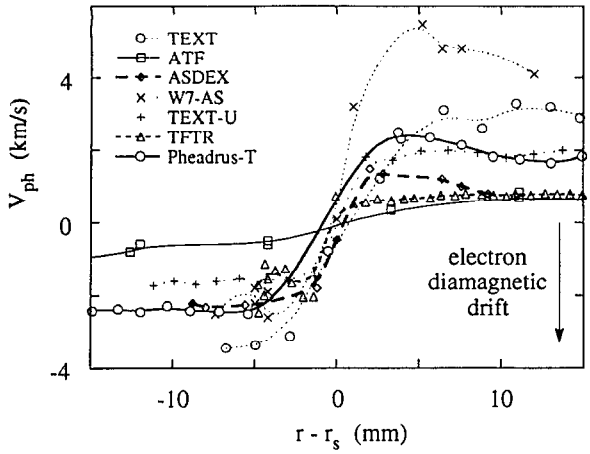

FIG. 1. Velocity shear layer depicted by the phase velocity (V_{ph}) of the turbulence. The profiles are aligned to the inversion point (r_s) where V_{ph} is zero.

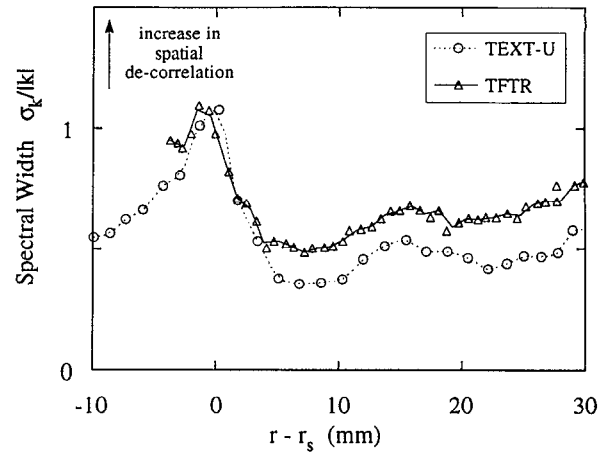

FIG. 2. Profile of the normalized spectral width ($\sigma_k/|k|$) in TEXT-U and TFTR showing increases within the shear layer. These are not H-mode plasmas.

the scrape-off region, the turbulence propagates in the ion diamagnetic drift direction. An interesting observation is that the thickness of the layer, typically 5–10 mm wide, appears to be rather insensitive to the differences in machine size, edge plasma parameters, and limiter configurations. Typically, the $\mathbf{E}\times\mathbf{B}$ velocity shear $dV_{\mathbf{E}\times\mathbf{B}}/dr$ ($\approx dV_{ph}/dr$) is in the range of 10^5–10^6 $\sec^{-1}$ in these experiments.

Theoretical studies[32–37] indicate that the velocity shear (or more appropriately the radial electric field shear) can influence the turbulence and the linear growth rate when the shear frequency $\omega_s = k_\perp \Delta_r dV_{\mathbf{E}\times\mathbf{B}}/dr$) is large compared to the diffusion rate τ_D^{-1} ($=D\Delta_r^{-2}$) or c_s/L_s. Using the radial correlation length or the mode width for Δ_r and the effective radial diffusion coefficient for D, it is found that the shear frequency is typically comparable or larger than both the diffusion rate and the ratio c_s/L_s in these experiments. Thus, it may be expected that the differential $\mathbf{E}\times\mathbf{B}$ rotation can "shear" apart the turbulence structure. When this happens, one may expect a broader spectrum, i.e., an increase in the spectral width. Examples of normalized spectral width ($\sigma_k/|k|$) from two-point cross-correlation measurements in TEXT-U and in TFTR in Fig. 2 show increases within the shear layer. In this region increase in $\sigma_k/|k|$ arises mostly from changes in σ_k. The increase in spectral width implies an increase in the spatial decorrelation and supports the idea of "shearing" of turbulence structure; a result consistent with previous observation in terms of correlation times in TEXT.[38] Reductions in the level of fluctuations in the proximity of the shear layer have also been observed in some cases. It has been suggested that shear decorrelation plays a role in H-mode plasmas, making the study in ordinary discharges very important.

III. EDGE TURBULENCE CHARACTERISTICS

A significant level of fluctuations with normalized rms amplitude of the order 10^{-1} exists in the edge plasma (in the vicinity of the last-closed flux surface) of all three device types. After taking into account superficial differences in the appearance, such as those arising from the orientation of the equilibrium magnetic field and the equilibrium $\mathbf{E}\times\mathbf{B}$ Doppler shift in the mode frequency, notable similarities in the turbulence characteristics are observed. In this section we present examples to illustrate how edge fluctuations are categorized in this comparative study, identify some of the commonly observed properties and discuss their implications, and investigate the electrostatic and electromagnetic nature of the fluctuations.

A. Categorizing edge fluctuations

In all three device types, there is a rich spectrum of intrinsic fluctuations. When comparing fluctuations between these devices, it is important to only compare similar kinds. For instance, strong MHD (magnetohydrodynamics) activity can lead to density fluctuation via ideal flux surface perturbation. Away from their resonant surfaces the MHD modes behave ideally and can give rise to density fluctuations via coupling to the equilibrium gradient, i.e.,

$$\frac{d\tilde{n}}{dt} = \frac{i}{\mathbf{k}\cdot\mathbf{B}_0}\frac{\partial n_0}{\partial r}\frac{d\tilde{B}_r}{dt}. \tag{1}$$

In RFP's, a high level of magnetic activity originating from "tearing modes" resonant close to the magnetic axis is detectable in the edge. With $|\tilde{B}|/B$ in the order of 10^{-2}, the density fluctuation level of order $|\tilde{n}/n_0| \sim (a/L_n)|\tilde{B}_r/B_0| \sim 10^{-1}$ indicates significant coupling to MHD perturbations in RFP's.[10] On the other hand, the density fluctuation of order $|\tilde{n}/n_0| \sim (L_s/k_\perp L_n\Delta_r)|\tilde{B}_r/B_0| \sim 10^{-2}$ for a magnetic fluctuation level of 10^{-5} as is found in tokamaks is negligible in the edge plasmas. The same conclusion is obtained for stellarators. This type of "frozen-in" perturbation does not cause particle transport. Therefore, it may be necessary to distinguish these global perturbations in the discussion of transport related phenomena.

An example of categorizing fluctuations, typical spectra of the ion saturation current fluctuation (I_{sat}) in the

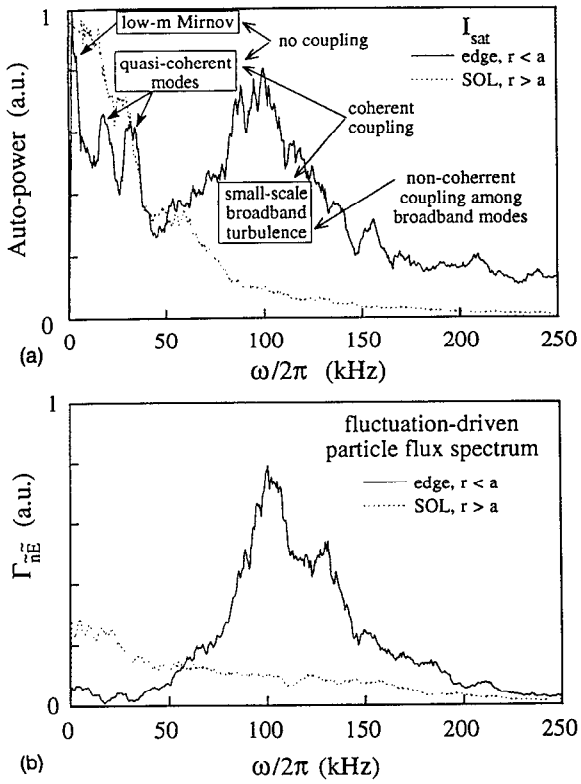

FIG. 3. Spectra of edge fluctuations ($\tilde{I}_{sat}$) [(a)] and the fluctuation-driven particle flux [(b)] in TEXT. In between the peak at the Mirnov frequency and the broadband activity are isolated peaks observable in spectra obtained near major resonant surfaces.

tokamak TEXT are shown in Fig. 3(a). The difference in the appearance of the two spectra, one taken in the scrape-off layer (represented by the dotted line) and the other taken in the bulk edge plasma inside the last-closed flux surface (represented by the solid line), can be largely attributed to the **E×B** rotation. The larger **E×B** Doppler shift in the bulk edge ($r<a$) helps to spread out the spectrum. In this case we can identify a peak at the low-m Mirnov frequency and a broadband high-frequency activity. In between these two spectral regions, isolated spectral peaks often exist in the power spectra obtained from fluctuation measurements near major resonant surfaces. These modes are labeled as quasicoherent modes[39] because they are less coherent than the Mirnov oscillations and are more coherent than the microturbulence. A comparison with the particle flux spectrum, shown in Fig. 3(b), indicates that the fluctuation-driven particle flux is mostly supported by the small-scale broadband turbulence. Using a bispectral analysis[40] which quantifies nonlinear three-wave coupling, we found that the quasicoherent modes are nonlinearly coupled to the broadband modes.[41] On the other hand, modes at the Mirnov frequency are neither coupled to the quasicoherent modes nor the broadband activity in normal discharges. This means that the relatively low-frequency, long-wavelength modes localized at major resonant surfaces in the edge region are indeed part of the edge turbulence. This result also indicates that radial mode structure is relevant in modeling the edge turbulence.

TABLE III. Edge fluctuation properties commonly observed in the experiments.

Property	Implication
non-Boltzmann; $\lvert\tilde{p}_e\rvert/p_e \neq \lvert e\tilde{\varphi}_{pl}\rvert/T_e$	nonadiabatic; resistive dissipation
$\lvert\tilde{n}\rvert/n > \lvert T_e\rvert/T_e$	not thermally driven; possible $\chi_\parallel$ influence
$k_\perp \rho_s \sim 10^{-1}$	simple drift waves have $k_\perp \rho_s \sim O[1]$
$\lvert\tilde{n}\rvert/n \sim (kL_n)^{-1}$	consistent with mixing length type of arguments

B. Commonly observed properties

Despite the vast differences among devices, some turbulence properties are commonly observed in both the scrape-off region and in the bulk edge plasma just inside the last-closed flux surface (see Table II and Ref. 7). They are summarized in Table III. The observations are by no means universal and there are exceptions. For instance, in the Madison Symmetric Torus[42] (MST) reversed-field pinch the fluctuations were found[5] not to depart from the simple Boltzmann relationship; in the tokamak TJ1[43] the normalized electron temperature fluctuation level is comparable or larger than that of the density; TFTR has even a lower value of $k_\perp \rho_s$; and the simple density scaling fails when edge plasma is perturbed by limiter biasing.

According to the simple parallel Ohm's without the thermal force term $\eta \tilde{j}_\parallel = -i\omega\tilde{A}_\parallel - \nabla_\parallel (\tilde{\varphi} - \tilde{p}_e/en)$, edge fluctuations which do not follow the simple Boltzmann relationship indicates nonadiabatic behavior, i.e., resistive dissipation can play a role. When the normalized fluctuation level of electron temperature is smaller than that of the density, thermal drive is not likely to be the principal driving mechanism. It also suggests possible influence from electron thermal conduction along the field lines. In these experiments (see Table II), $k_\perp \rho_s$ typically is about 0.1. This is an order of magnitude smaller than that expected from simple drift wave theories. In a number of cases, when measurements are available, it is estimated that the collisionality parameter[44] ($k_\parallel^2 v_{th}^2/\omega\nu_e \sim k_\parallel^2 \chi_\parallel/\omega$ with $k_\parallel = k_\perp \Delta_r/L_s$) for the edge turbulence is of order unity, i.e., the modes are semicollisional. This parameter is a measure of the electron parallel diffusion over one wave period. When it is comparable to or larger than unity, electron thermal conduction along the field lines can stabilize mode growth and lead to saturation. It also implies effects of radial mode structure in sheared magnetic field. In a very general sense, we find that the normalized density fluctuation level scales inversely with $k_\perp L_n$. This appears to support the argument that if density gradients drive the turbulence, the drive stops when the density gradient is locally flattened. Another common feature in these measurement is the proximity to the open field lines. With the large range of possible linear drive mechanisms (e.g., I_p and curvature), different edge configurations (e.g., divertor and limiter types), and variations in edge conditions (e.g., Z_{eff} and level and mix of impurities) represented, it

was not possible to associate the general observations with any one single instability drive. It would seem that the commonly observed characteristics could be signatures of the plasma dynamics connected to the nonlinear saturation process. Further investigation is also needed to determine if open field line effects are important.

C. Are edge fluctuations purely electrostatic?

Fluctuations observed with Langmuir probes are often described as electrostatic. This description is useful to distinguish the transport associated with these fluctuations from that associated with stochastic magnetic fields. The electrostatic labeling may be slightly misleading in that the fluctuations themselves need not be purely "electrostatic," i.e., the electromagnetic component may contribute to the mode dynamics. According to the Ampère's law and the parallel Ohm's law, $(\eta/\mu_0)\nabla_\perp^2 \tilde{A}_\parallel = \eta \tilde{j}_\parallel = -\nabla_\parallel \tilde{\varphi} - i\omega \tilde{A}_\parallel$ where $\tilde{A}_\parallel$ is the fluctuating parallel magnetic potential and the time derivative is replaced by $i\omega$, the induced parallel electric field (i.e., $i\omega \tilde{A}_\parallel$) is negligible for purely electrostatic modes. In this case, the resistive dissipation is balanced by the parallel gradient of the electrostatic potential. (The parallel drive can be extended to include the electron pressure and the thermal force.) Thus, the electrostatic limit corresponds to $g \ll 1$ where the dimensionless parameter g is defined as the ratio of the induced electric field to the resistive drop, i.e.,

$$g = \frac{|\partial \tilde{A}_\parallel / \partial t|}{|\eta \tilde{j}_\parallel|} = \frac{\mu_0 \omega}{|\eta \nabla_\perp^2|}. \tag{2}$$

The parameter g, which describes the ratio of a "skin time" to the mode rotational time, can be estimated using two approaches. In the fine-scale electrostatic limit, $\nabla_\perp^2$ is replaced with the measured $k_\perp^2$ to give an upper bound g_1. In the other, an estimate of the magnetic mode width, taken to be $3\rho_s$, is used to give a lower bound g_2. The frequency ω is taken to be the electron diamagnetic drift frequency. This is deemed appropriate, even though ω is much reduced when diamagnetic effects are included in the linear theory, because there are $\chi_\parallel$ effects and turbulence broadening. The estimates of the upper bound g_1 (solid symbols) and lower bound g_2 (open symbols) are plotted in Fig. 4. This figure shows the radial behavior for data obtained in TEXT (with an error bar denoting the standard error of the mean) as well as estimates near the plasma edge for some other devices. The values of g in the scrape-off layer are generally much less than unity indicating that the fluctuations can be described as "electrostatic." Inside the last-closed flux surface, the indication from TEXT data as well as from other machines including ZT-40M, Phaedrus-T, and TFTR is that the electromagnetic contribution is not negligible. For the pinch ZT-40M, the results are not unexpected because of the high level of magnetic activity observed.

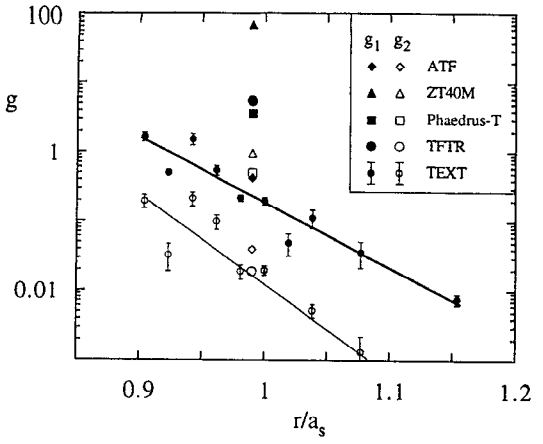

FIG. 4. Profiles of the parameter g in TEXT and estimates near the plasma edge in some other devices. Solid symbols represent the upper bound g_1 and open symbols the lower bound g_2. Fluctuations can be regarded as "electrostatic" when $g \ll 1$. Error bar shown is the standard error of the mean.

IV. FLUCTUATION-DRIVEN TRANSPORT

The role of fluctuations in edge transport can be assessed by comparing the fluctuation-driven fluxes with those estimated from equilibrium measurements using a simple scrape-off layer model.[45] It is important to recognize that significant asymmetries exist in the scrape off layer,[46] so that such comparison cannot be exact and at best reflects local rather than global balance.

When the local source of particles can be ignored, balancing the parallel loss to the limiter with the radial variation of the outward flux $(\partial \Gamma_x/\partial x + nc_s/2L_c \approx 0)$ yields the total radial flux, i.e.,

$$\Gamma_{\mathrm{SOL}} \approx 0.5 n c_s \lambda / L_c, \tag{3}$$

where $\lambda^{-1} = L_n^{-1} + 0.5 L_{T_e}^{-1}$ and L_c is the characteristic connection length to a limiter. For this simple estimate to be meaningful, it is necessary to check the validity of certain assumptions such as the exponential falloff of equilibrium density and temperature profiles, small scale length λ relative to the scrape-off layer width, and ignorable local source. Figure 5 shows a comparison between the measured electrostatic turbulence-driven particle flux $\Gamma_{\tilde{n}\tilde{E}}$ and the total radial flux Γ_{SOL} derived from Eq. (3) simultaneously at the same location. Within the typical experimental variations, they agree reasonably well over a fairly wide range. There are exceptions. For instance, the data from a discharge with typical edge q value ($=3.5$) in Tokapole[47] follow the trend. Yet, data from a discharge with low edge q value ($=1.4$) behave quite differently. In the lower edge q case, both the assumptions of exponential falloff profile and small λ are not well satisfied and there is high level of magnetic activity. Nevertheless, the large departure of this data from the trend is not fully understood. The conclusion from this comparison is that generally the fluctuation-driven particle flux can explain the density behavior in the scrape-off layer.

When the local source of particles as well as the local source and sink of electron energy can be ignored, the balance of the radial energy flow to the parallel energy loss to the limiter is

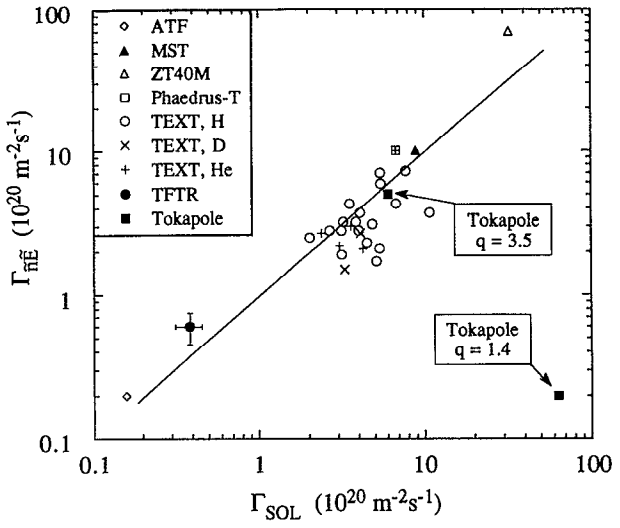

FIG. 5. A comparison between the turbulence-driven particle flux ($\Gamma_{\tilde{n}\tilde{E}}$) from density and perpendicular electric field correlation measurement and the estimates of total radial flux (Γ_{SOL}) from equilibrium parameters in the scrape-off layer.

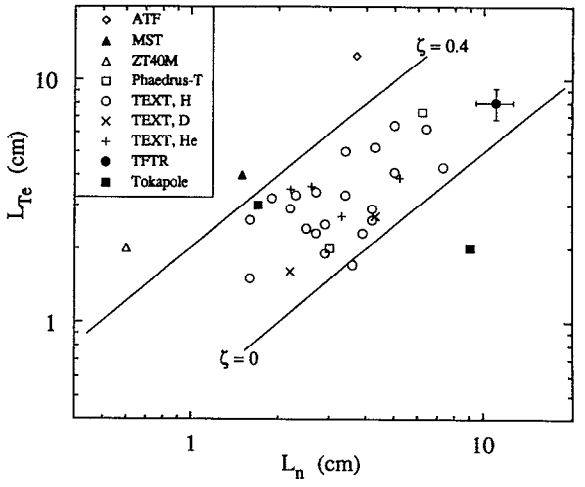

FIG. 6. Behavior of the electron temperature scale lengths (L_{Te}) versus the density scale lengths (L_n). Constant ratio of conductive to connective electron energy flux (ζ) corresponds to straight lines as depicted by the two lines for $\zeta=0$ and 0.4.

$$\frac{5\partial T_e\Gamma_x}{2\partial x}+\frac{\partial q_x}{\partial x}\approx\frac{\gamma_{\|}\, nc_sT_e}{2L_c}, \tag{4}$$

where the first and second term on the right-hand side of Eq. (4) are the radial connective and conductive energy flux, respectively, and $\gamma_{\|}$ is the electron parallel energy transmission coefficient. From the above equation, the ratio of energy conduction to energy convection ζ can be related to the electron temperature and density scale lengths:

$$\zeta=\frac{2}{5}\gamma_{\|}\,\frac{(L_{T_e}/L_n)+\frac{1}{2}}{(L_{T_e}/L_n)+\frac{3}{2}}-1. \tag{5}$$

Using a typical value of $\gamma_{\|}=5$, the above expression gives $\zeta\approx0.4$ when $L_{T_e}/L_n = 2$ and $\zeta=0$ when $L_{T_e}/L_n = 1/2$. Measurements of the fluctuation-driven energy flux indicate that in tokamaks the conductive energy flux is typically 20% to 40% of the connective energy flux ($\zeta=0.2$–0.4) while in pinches magnetic turbulence explains energy transport with electrostatic turbulence explaining particle transport (i.e., $\zeta\gg1$). These results can be tested against the behavior of electron temperature and density scale lengths. In Fig. 6, where the electron temperature scale length is plotted against the density scale length, the two straight lines correspond to no conductive energy flux ($\zeta=0$) with conductive energy flux being 40% of connective energy flux ($\zeta=0.4$). Most tokamak data fall in between these two lines. This means that the scale length behavior is consistent with the measured energy flux ratio. For the stellarator ATF and pinches MST and ZT-40M data, it seems that conduction is large. This is expected for the pinch data because the high level of magnetic fluctuations can lead to large conductive energy flux. The ATF result might be explained by the presence of a stochastic magnetic field associated with the destruction of the separatrix.

V. CONCLUSIONS

A velocity shear layer has been found, in a number of different edge configurations, in the edge plasmas of tokamaks and stellarators but not of RFP's. There is sufficient velocity shear and shear decorrelation in these non-H-mode shear layers to investigate their role on turbulence and transport. The necessity and means to categorizing edge fluctuations are discussed. A comparison of the fluctuations over a wide range of parameters reveals some generic properties of the turbulence. The typical amplitude ordering of $e|\tilde{\varphi}_{pl}|/T_e > |\tilde{n}|/n > |\tilde{T}_e|/T_e$ indicates that thermal drive is not likely the principal mechanism to sustain these non-Boltzmann fluctuations. It is found that electron parallel thermal conduction can play a role in the saturation process and that radial mode structure and the electromagnetic component of the fluctuations are both relevant to the turbulence dynamics. Further study is needed to determine if open field-line effects are important. Turbulence is pertinent to edge transport: electrostatic turbulence can explain the particle transport in all three device types and the thermal transport in tokamaks.

This study addresses only some of the elementary issues of edge turbulence and transport. Many other remain to be resolved; for instance, the effect of asymmetries, plasma flow, and open field lines. The use of controlled perturbation can help reveal the properties and the origin of the turbulence. It is expected that the application of higher-order fluctuation analysis (e.g., bispectral analysis) can provide more insight into the dynamics. In addition to the collection of data presented here, a wealth of edge turbulence measurements on many other devices exists. A consolidation of these measurements could be used to val-

idate (or otherwise) various proposed driving mechanisms for the observed turbulence and tranpsort, and to provide empirical scaling laws for parameters useful in machine design.

ACKNOWLEDGMENTS

We would like to thank the operating staff of all machines concerned, without whom this work could not have been performed, and L. Giannone, P. Grigull, K. McCormic, H. Niedermeyer for data from W7-AS and ASDEX.

The data taking and analysis were supported by the U.S. Department of Energy, Office of Fusion Energy, Grant No. DE-FG05-89ER-53295.

[1]J. D. Callen, B. A. Carreras, and R. D. Stambaugh, Phys. Today **45** (1), 34 (1992).
[2]A. J. Wootton, B. A. Carreras, H. Matsumoto, K. McGuire, W. A. Peebles, Ch. P. Ritz, P. W. Terry, and S. J. Zweben, Phys. Fluids B **2**, 2879 (1990).
[3]T. Uckan, C. Hidago, J. D. Bell, J. H. Harris, J. L. Dunlap, J. B. Wilgen, Ch. P. Ritz, T. L. Rhodes, and A. J. Wootton, Phys. Fluids B **3**, 1000 (1991).
[4]H. Ji, H. Toyama, K. Miyamoto, S. Shinohara, and A. Fujisawa, Phys. Rev. Lett. **67**, 62 (1991).
[5]T. D. Rempel, C. W. Spragins, S. C. Prager, S. Assadi, D. J. Den Hartog, and S. Hokin, Phys. Rev. Lett. **67**, 1438 (1991).
[6]A. Howling, A. W. Morris, and D. C. Robinson, in *Magnetic Reconnection and Turbulence* (Ecole Polytechnique, Palaiseau, France, 1985), p. 329.
[7]H. Y. W. Tsui, H. Lin, M. Meier, C. Ritz, and A. J. Wootton, in *Proceedings of the 18th European Conference on Controlled Fusion and Plasma Physics,* Berlin (European Physical Society, Geneva, 1991),Vol. 15C, Part I, p. 297; H. Y. W. Tsui, A. J. Wootton, J. D. Bell, R. D. Bengtson, D. Diebold, J. H. Harris, H. Hershkowitz, C. Hidalgo, J. C. Ingraham, G. X. Li, H. Lin, S. C. Luckhardt, D. M. Manos, M. A. Meier, G. M. Miller, C. P. Munson, J. Pew, Ch. P. Ritz, A. Rudyj, K. F. Schoenberg, J. Sorensen, T. Tanaka, and T. Uckan, J. Nucl. Mater. **196–198**, 794 (1992); A. J. Wootton, H. Y. W. Tsui, and S. Prager, Plasma Phys. Controlled Fusion **34**, 2023 (1992).
[8]C. P. Ritz, T. L. Rhodes, H. Lin, W. L. Rowan, H. Tsui, M. Meier, R. D. Bengtson, A. J. Wootton, B. A. Carreras, J.-N. Leboeuf, D. K. Lee, J. H. Harris, C. Hidalgo, J. D. Bell, J. A. Holmes, R. C. Isler, V. E. Lynch, T. Uckan, P. H. Diamond, A. S. Ware, and D. R. Thayer, in *Plasma Physics and Controlled Nuclear Fusion Research, 1990* (International Atomic Energy Agency, Vienna, 1991), Vol. 2, p. 589.
[9]Ch. P. Ritz, H. Y. W. Tsui, T. L. Rhodes, R. D. Bengtson, H. Lin, and A. J. Wootton, Rev. Sci. Instrum. **61**, 2998 (1990).
[10]H. Y. W. Tsui, Ch. P. Ritz, G. Miller, J. C. Ingraham, C. P. Munson, K. F. Schoenberg, and P. G. Weber, Nucl. Fusion **31**, 2371 (1991).
[11]D. Diebold, N. Hershkowitz, J. Pew, J. Sorensen, T. Tanaka, and H. Y. W. Tsui, Ch. P. Ritz, and A. J. Wootton, J. Nucl. Mater. **196–198**, 789 (1992).
[12]H. Y. W. Tsui, D. M. Manos, A. Rudyj, Ch. P. Ritz, and A. J. Wootton, J. Nucl. Mater. **196–198**, 292 (1992).
[13]J. F. Lyon, B. A. Carreras, K. K. Chipley, M. J. Cole, J. H. Harris, T. C. Jernigan, R. L. Johnson, V. E. Lynch, B. E. Nelson, J. A. Rome, J. Sheffield, and P. B. Thompson, Fusion Technol. **10**, 179 (1986).
[14]R. S. Massey, R. G. Watt, P. G. Weber, G. A. Wurden, D. A. Baker, C. J. Buchenauer, L. C. Burkhardt, T. Cayton, J. N. DiMarco, J. N. Downing, R. M. Erickson, R. F. Gribble, A. Haberstich, R. B. Howell, J. C. Ingraham, E. M. Little, G. Miller, C. P. Munson, J. A. Phillips, M. M. Pickrell, K. F. Schoenberg, A. E. Schofield, and D. M. Weldon, Fusion Technol. **8**, 1571 (1985).
[15]D. A. Diebold, R. Majeski, T. Tankan, J. Sorensen, J. Pew, N. Hershkowitz, R. A. Breun, G. McKee, J. Meyer, P. H. Probert, and G. Winz, Nucl. Fusion **32**, 2040 (1992).
[16]K. W. Gentle, Nucl. Technol. Fusion **1**, 479 (1981).
[17]D. M. Meade, V. Arunasalam, C. W. Barnes, M. G. Bell, R. Bell, M. Bitter, R. Boivin, N. L. Bretz, R. Bundy, C. E. Bush, A. Cavallo, C. Z. Cheng, T. K. Chu, S. A. Cohen, S. Cowley, S. L. Davis, D. L. Dimock, J. Dooling, H. F. Dylla, P. C. Efthimion, A. B. Ehrhardt, R. J. Fonck, E. Fredrickson, H. P. Furth, R. J. Goldston, G. Greene, B. Grek, L. R. Grisham, G. Hammet, R. J. Hawryluk, K. W. Hill, J. Hosea, R. B. Howell, R. A. Hulse, H. Hsuan, A. Janos, D. Jassby, F. C. Lobes, D. W. Johnson, R. Kaita, S. Kaye, J. Kesner, C. Kieras-Phillips, S. J. Kilpatrick, H. Kugel, P. H. LaMarche, B. LeBlanc, D. M. Manos, D. K. Mansfield, E. S. Marmar, E. Mazzucato, M. P. McCarthy, M. Mauel, D. C. McCune, K. M. McGuire, S. S. Medley, D. R. Mikelsen, D. Monticello, R. Motley, D. Mueller, J. Murphy, Y. Nagayama, G. A. Navrtail, R. Nazikian, D. K. Owens, H. Park, W. Park, S. Paul, R. Perkins, S. Pitcher, A. T. Ramsey, M. H. Redi, G. Rewoldt, D. Roberts, A. L. Roquemore, P. H. Rutherford, S. Sabbagh, G. Schilling, J. Schivell, G. L. Schmidt, S. D. Scott, J. Snipes, J. Stevens, J. D. Strachan, B. C. Stratton, W. Stodick, E. Synakowshi, W. Tang, G. Taylor, J. Terry, J. R. Timberlake, H. H. Towner, M. Ulrickson, S. von Goeler, R. Wieland, M. Williams, J. R. Wilson, K. L. Wong, M. Yamada, S. Yoshikawa, K. M. Young, M. C. Zarnstorff, and S. J. Zweben, in Ref. 8, Vol. 1, p. 9.
[18]S. Chen, and T. Sekiguchi, J. Appl. Phys. **36**, 2363 (1965).
[19]H. Y. W. Tsui, R. D. Bengston, G. X. Li, H. Lin, M. Meier, Ch. P. Ritz, and A. J. Wootton, Rev. Sci. Instrum. **63**, 4608 (1992).
[20]J. M. Beall, Y. C. Kim, and E. J. Powers, J. Appl. Phys. **53**, 3933 (1982).
[21]D. W. Ross, Comments Plasma Phys. Controlled Fusion **12**, 155 (1989).
[22]J. F. Drake, Phys. Fluids **30**, 2429 (1987).
[23]D. R. Thayer and P. H. Diamond, Phys. Rev. Lett. **65**, 2784 (1990).
[24]J.-N. Leboeuf, D. K. Lee, B. A. Carreras, N. Dominguez, P. H. Diamond, A. S. Ware, Ch. P. Ritz, A. J. Wootton, W. L. Rowan, and R.V. Bravenec, Phys. Fluids B **3**, 2291 (1991); A. S. Ware, P. H. Diamond, H. Biglari, B. A. Carreras, L. A. Charlton, J.-N. Leboeuf, and A. J. Wootton, Phys. Fluids B **4**, 877 (1992).
[25]M. A. Beer and T. S. Hahm, Phys. Fluids B **4**, 2567 (1992).
[26]H. L. Berk, D. D. Ryutov, and Yu. A. Tsidulko, Phys. Fluids B **3**, 1346 (1991).
[27]A. V. Nedospasov, J. Nucl. Mater. **196–198**, 90 (1992).
[28]R. D. Hazeltine, Phys. Fluids B **1**, 2031 (1989).
[29]H. Y. W. Tsui, Phys. Fluids B **4**, 4057 (1992).
[30]P. H. Diamond and Y. B. Kim, Phys. Fluids B **3**, 1626 (1991).
[31]B. A. Carreras, V. E. Lynch, and L. Garcia, Phys. Fluids B **3**, 1438 (1991).
[32]K. C. Shaing and E. C. Crume, Jr., Phys. Rev. Lett. **63**, 2369 (1989).
[33]Y. B. Kim, P. H. Diamond, H. Biglari, and P. W. Terry, Phys. Fluids B **2**, 2143 (1990).
[34]H. Biglari, P. H. Diamond, and P. W. Terry, Phys. Fluids B **2**, 1 (1990).
[35]S. Hamaguchi and W. Horton, Phys. Fluids B **4**, 319 (1992).
[36]Y. Z. Zhang and S. M. Mahajan, Phys. Fluids B **5**, 2000 (1993).
[37]A. B. Hassam, Comments Plasma Phys. Controlled Fusion **14**, 275 (1992).
[38]Ch. P. Ritz, H. Lin, T. L. Rhodes, and A. J. Wootton, Phys. Rev. Lett. **65**, 2543 (1990).
[39]H. Y. W. Tsui, P. M. Schoch, and A. J. Wootton, Phys. Fluids B **5**, 1274 (1993).
[40]Y. C. Kim and E. J. Powers, IEEE Trans. Plasma Sci. **PS-7**, 120 (1979).
[41]H. Y. W. Tsui, K. Rypdal, Ch. P. Ritz, and A. J. Wootton, Phys. Rev. Lett. **70**, 2565 (1993).
[42]R. N. Dexter, D. W. Kerst, T. W. Lovell, S. C. Prager, and J. C. Sprott, Fusion Technol. **19**, 131 (1991).
[43]C. Hidalgo, R. Bolbin, M. A. Pedrosa, I. Garcia-Cortes, and M. A. Ochando, Phys. Rev. Lett. **69**, 1205 (1992).
[44]C. S. Chang, R. R. Dominguez, and R. D. Hazeltine, Phys. Fluids **24**, 1655 (1981).
[45]P. C. Stangeby and G. M. McCracken, Nucl. Fusion **30**, 1225 (1990).
[46]G. R. Tynan, L. Schmitz, R. W. Conn, R. Doerner, and R. Lehmer, Phys. Rev. Lett. **68**, 3032 (1992).
[47]I. H. Tan and S. C. Prager, Phys. Rev. Lett. **68**, 1714 (1992).